JOURNAL OF NEUROPHYSIOLOGY
Vol. 71, No. 2, February 1994. *Printed in U.S.A.*

Modulation of High-Threshold Transmission Between Heart Interneurons of the Medicinal Leech by FMRF-NH_2

TED W. SIMON, JOACHIM SCHMIDT, AND RONALD L. CALABRESE
Department of Biology, Emory University, Atlanta, Georgia 30322

SUMMARY AND CONCLUSIONS

1. We examined high-threshold synaptic transmission between oscillatory pairs of leech heart interneurons. Inhibitory postsynaptic currents (IPSCs) could be reliably evoked by depolarizing the presynaptic neuron in voltage clamp from a holding potential of −35 mV. At this presynaptic potential, the Ca^{2+} currents underlying graded transmission are completely inactivated, and we conclude that a high-threshold Ca^{2+} current is extant in heart interneurons. Further evidence for this was that inhibitory postsynaptic currents were blocked when Co^{2+} replaced Ca^{2+} in the saline and thus high-threshold transmission was dependent on the presence of external Ca^{2+}.

2. When IPSCs were evoked by a 200-ms duration voltage step from a holding potential of −35 mV in the presynaptic neuron, the time course of turn-on of the IPSC consisted of a fast (time-to-peak = 17.5 ± 1.93 (SE) ms [n = 7]) and a slow (time-to-peak = 250 ± 28.5 ms [n = 8]) component. FMRF-NH_2 reduced the amplitude of the fast component but did not affect the slow component. When the presynaptic voltage step was ended the IPSC turned off with a single exponential time course. FMRF-NH_2 slowed the time course of turn-off of the IPSC.

3. When IPSCs were evoked by a 1500-ms duration voltage step from a holding potential of −35 mV in the presynaptic neuron, these IPSCs peaked around 300 ms. Following the peak, the IPSC decayed with a single exponential time course. FMRF-NH_2 accelerated the time course of this decay. At potentials of 0 mV and +5 mV, FMRF-NH_2 produced a significant decrease in the peak current and at potentials of −5 mV and 0 mV, produced a significant decrease in the current integral.

4. High-threshold IPSCs could also be evoked by a spike in the presynaptic neuron. Bath application of 1 μM FMRF-NH_2 decreased the amplitude of the spike-evoked IPSC and slowed the time course of its falling phase.

5. We examined the effect of FMRF-NH_2 on the quantal synaptic transmission. Bath-application of FMRF-NH_2 increased binomial p, the probability of release, and decreased binomial n, the number of units available for release. FMRF-NH_2 had no effect on q, the unit size, when calculated from the distributions of PSPs, and increased the coefficient of variation (CV).

6. The lack of a change in q and the increase in CV suggested that FMRF-NH_2 acted at a presynaptic location. We applied acetylcholine, the transmitter between heart interneurons, focally to the somata of these neurons and found that FMRF-NH_2 produced no change in the response of these cells to applied transmitter.

7. We produced a computer model of a heart interneuron having only a leak conductance, I_h, the hyperpolarization-activated inward current, and the high-threshold synaptic conductance. Results of the modeling suggest that FMRF-NH_2 may produce its effects on the heart rhythm by interactions of its effects on high-threshold transmission with both I_h and low-threshold Ca^{2+} currents.

INTRODUCTION

In the medicinal leech, seven bilateral pairs of heart interneurons comprise the heartbeat pattern generator that controls timing and coordination of the hearts in the absence of sensory feedback (Calabrese 1977; Thompson and Stent 1976). Each of the pairs of heart interneurons in the third and fourth segmental ganglia form reciprocal inhibitory synapses across the ganglionic midline (Peterson 1983). Normal electrical activity recorded from oscillatory pairs of heart interneurons consists of periods of inhibition (inhibited phase) alternating with depolarized plateaus and bursts of action potentials (plateau/burst phase) with a period of 6–15 s at room temperature (Calabrese et al. 1989; Thompson and Stent 1976).

During the normal rhythm, reciprocal inhibition between individual heart interneurons occurs by both low-threshold graded transmission and high-threshold spike-mediated transmission (Calabrese et al. 1989).

Low-threshold transmission occurs at presynaptic membrane potentials between −70 and −40 mV. Low-threshold Ca^{2+} currents begin to activate at ~ −60 mV, are completely inactivated at −45 mV, and contribute to the plateau in the plateau/burst phase (Angstadt and Calabrese 1991). Low-threshold transmission is graded with presynaptic membrane potential and has been correlated with these low-threshold Ca^{2+} currents (Angstadt and Calabrese 1991). Low-threshold transmission has a duration of between 3 and 8 s during the normal rhythm.

High-threshold transmission occurs at depolarized presynaptic potentials, −30 mV and above, and is normally mediated by action potentials. Because of this association with action potentials, high-threshold transmission normally has a much shorter duration (<50 ms) than low-threshold transmission and is expressed as discrete inhibitory postsynaptic potentials (IPSPs).

Stimulation of cell 204 that contains FMRF-NH_2-like immunoreactivity produces an acceleration of the leech heartbeat pattern generator (Arbas and Calabrese 1984). Similarly, exogenously applied FMRF-NH_2 can both accelerate the heart rhythm and also produce a disruptive response in which the heart rhythm is abolished (Kuhlman et al. 1985; Simon et al. 1992).

In the present study, we use both single electrode voltage clamp and discontinuous current clamp to examine high-threshold synaptic transmission (spike-mediated) between heart interneurons and the effect of FMRF-NH_2 on this type of transmission. We also examine the effect of FMRF-NH_2 on quantal synaptic transmission and the binomial

parameters, n, p, and q (e.g., Korn and Faber 1991; Maclachlan 1978). We use a computer model to examine the interaction of high-threshold transmission and I_h, the hyperpolarization-activated inward current (Angstadt and Calabrese 1989). These results suggest that the disruptive response to FMRF-NH_2 is produced by reduction of IPSP amplitude and the acceleratory response to FMRF-NH_2 is caused by the broadening of IPSPs which in turn increases activation of I_h.

Whether these suggested mechanisms of action of FMRF-NH_2 will in fact account for the acceleratory and disruptive responses awaits their incorporation into the extant model of the elemental oscillator (DeSchutter et al. 1993a).

MATERIALS AND METHODS

Animals and preparation

Leeches, *Hirudo medicinalis*, were obtained from Leeches USA (New York) and maintained in artificial pond water at 15°C. Animals were anesthetized in ice cold saline, and individual ganglia were dissected. Ganglia were pinned ventral side up in Sylgard (Dow-Corning) lined petri dishes (bath volume, 0.5 ml) and the connective tissue sheath over the neuronal somata was removed with fine scissors. We examined pairs of heart interneurons in segmental ganglia 3 and 4 and found no differences in synaptic transmission in different ganglia.

Solutions and electrodes

Ganglia were initially superfused (1.5 ml/min) with normal leech saline containing in mM: 115 NaCl, 4 KCl, 1.8 $CaCl_2$, 10 glucose, 10 *N*-2-hydroxyethylpiperazine-*N'*-2-ethanesulfonic acid (HEPES), pH 7.4. Depending on the experiment, the saline was changed to *1*) 0 Na^+, 115 *N*-methyl D-glucamine, 1.8 Ca^{2+}; *2*) 0 Na^+, 115 *N*-methyl D-glucamine, 0 Ca^{2+}, 1.8 Co^{2+}; *3*) 90 Na^+, 7.5 Ca^{2+}, 20 Mg^{2+}; or *4*) 90 Na^+, 5 Ca^{2+}, 20 Mg^{2+}. [Cl^-] was not measured in the salines but was estimated between 120 and 140 mM.

FMRF-NH_2 (BaChem, Peninsula) was dissolved in HPLC grade water (VWR) at a concentration of 5 mg/ml, stored frozen and diluted in saline immediately prior to use. FMRF-NH_2 was bath-applied at 1 μM in all experiments. The concentration of acetylcholine focally applied to heart interneuron somata was 1 mM (Schmidt and Calabrese 1992).

Intracellular recordings were made with borosilicate microelectrodes (1 mm, OD, 0.75 mm, ID) filled with 4 M K-acetate with 20 mM KCl (25–35 MΩ). Addition of this small amount of KCl improved the current-passing qualities of these electrodes and is routine in our laboratory.

Experimental protocol for voltage clamp

Pre- and postsynaptic currents were measured with two switching single electrode voltage clamps (Axoclamp 2A, Axon Instruments, Foster City, CA). In single electrode voltage clamp mode, the voltage input to the sample and hold circuit was monitored to ensure complete electrode settling between current injection cycles. Sample rates ranged between 2.5 and 6 kHz and clamp gain from 8 to 25 nA/mV. The output bandwidth was either 0.3 or 1 kHz with higher and lower sample rates, respectively. The sampling frequency of one voltage clamp (slave) was driven by the clock of the other clamp (master). Voltage clamp data were digitized and later analyzed using a personal computer and PCLAMP software (Axon Instruments).

In some experiments (Figs. 5, 8–10), one or both neurons were held in discontinuous current clamp. In most experiments both neurons were held at −35 mV unless otherwise stated.

For convenience and accuracy, we will refer to postsynaptic currents measured with the postsynaptic neuron under voltage clamp and evoked by a spike in the presynaptic neuron held under discontinuous current clamp as spike-evoked IPSCs. We will refer postsynaptic currents also measured with the postsynaptic neuron under voltage clamp evoked by a depolarizing step in the presynaptic neuron held under voltage clamp as step-evoked IPSCs.

Experimental protocol for quantal analysis

Quantal analysis experiments were performed in saline containing (in mM) either 90 Na^+, 7.5 Ca^{2+}, and 20 Mg^{2+}, or 90 Na^+, 5 Ca^{2+}, and 20 Mg^{2+}. Presynaptic spikes were triggered by a suprathreshold current pulse ranging from 0.2 to 1 ms in duration at a rate of 1 Hz. Both pre- and postsynaptic membrane potentials were measured using discontinuous current clamp (DCC) at sample rates ranging from 2 to 7 kHz and recorded on a VHS video recorder modified for FM recording (Vetter Instruments, Chambersburg, PA). Pre- and postsynaptic membrane potentials were digitized and analyzed offline with PCLAMP software (Axon Instruments).

The arrays of IPSPs used for quantal analysis consisted of between 96 and 190 individual responses. These data were obtained from nine pairs of heart interneurons. We determined the point of minimum latency from examination of at least twenty of the largest IPSPs from a particular experiment (Fig. 8*B*). The average latency from the peak of the presynaptic spike to the point of minimum latency was 2.9 ± 0.6 ms (n = 9). IPSP amplitudes were measured as the difference in potential between the point of minimum latency and the peak of the IPSP occurring within 20 ms from the point of minimum latency (Fig. 8*B*). For convenience, the sign of the IPSPs was reversed so that hyperpolarizing responses appear to the right along the abscissa and depolarizing responses appear to the left (e.g., Nicholls and Wallace 1978). The IPSPs were placed into bins 0.05 mV wide.

The presynaptic neuron was held at either −40, −35, or −30 mV. In five of the nine experiments, an array of IPSPs with the presynaptic neuron held at −50 mV (Fig. 8*A*) was also collected and used to estimate q, the unit size. Synaptic transmission and quantal content were reduced with the presynaptic neuron hyperpolarized (Nicholls and Wallace 1978). In these five experiments, Poisson assumptions (i.e., high n and low p) were used to determine m, quantal content, from the method of failures. We assumed that the number of failures equaled the number of "zeroes" (response with a flat postsynaptic voltage response) plus twice the number of depolarizing responses (m_{failures}) (e.g., Nicholls and Wallace 1978; Fig. 9*C*). To calculate q, the unit size from these responses, we considered all depolarizing responses equal to zero and used

$$q = \frac{\bar{v}}{m_{\text{failures}}} \qquad (1)$$

where $\bar{v}$ = mean of all PSPs

The variance of the unit size, σ_q^2, was determined from the responses taken with the presynaptic neuron held at −50 mV by choosing an upper and lower limit for the singles and calculating the variance of the amplitudes of the IPSPs falling within these limits. We used these values of q and σ_q^2 as values for estimating the unit size for arrays of IPSPs taken at −40 and −30 mV.

In the four experiments from which no data was available with the presynaptic neurons held at −50 mV, we chose an upper and lower limit for the singles and calculated the mean and variance within those limits. Our estimates of the unit size were within the range of 0.3 to 0.6 mV similar to the values measured by Nicholls and Wallace (1978).

TABLE 1. *Effects of FMRF-NH_2 on the parameters of the spike-evoked postsynaptic current*

Parameter	Normal	FMRF-NH_2
IPSC Amplitude, pA	165 ± 56	69 ± 43 $t_{s[6,2]} = 3.03$ $P < 0.02$
Falling phase τ, ms	10.75 ± 3.94	16.97 ± 6.59 $t_{s[6,2]} = 2.23$ $P < 0.05$

Values are means ± SE. IPSC, inhibitory postsynaptic current.

In all nine instances of arrays of IPSPs collected with the presynaptic neuron held at −30 to −40 mV, the number of failures was low indicating that the probability of release was high and that binomial rather than Poisson analysis was appropriate. In these experiments, we measured quantal content directly as the ratio between the total number of quanta released and the total number of responses in the array of IPSPs (e.g., Johnson and Wernig 1971)

$$m = \frac{\sum \frac{\text{IPSPamplitude}}{q}}{N} \quad (2)$$

where N = total number of IPSPs

From this estimate of m, we calculated binomial p and n as follows (Maclachlan 1978)

$$p = 1 - \frac{S^2}{m} \quad (3)$$

where S^2 = variance of the quantal content of the IPSP array with depolarizing responses = 0.0 and

$$n = \frac{m}{p} \quad (4)$$

The standard error of binomial n was calculated as

$$SE_n = \sqrt{\frac{2n(n-1)(1-p)^2}{Np^2}} \quad (5)$$

An integer value was chosen for binomial n within one standard error of the value calculated from *Eq. 4*. Binomial p was then recalculated from *Eq. 4*. Sums of gaussian distributions weighted by the appropriate binomial weights, given n, p, and q previously calculated were fitted to the histograms of IPSP amplitudes. Chi-square tests were used to determine goodness of fit.

Noise analysis was performed on a pair of cells in which the stimulating current delivered to the presynaptic neuron was below-threshold (Fig. 8*C*). We did not correct for the noise in the histograms of the IPSPs and thus introduced a small inaccuracy when calculating S^2, p, and n. In all nine experiments the histograms were extremely well fit by our distributions (χ^2 probabilities >0.95).

No corrections for noise or the variability of individual quanta were made (Maclachlan 1978). Nonstationarity would cause binomial n to be underestimated (Brown et al. 1976). Because the values of binomial n we determined were generally small (<5, Table 1), we did not correct for nonstationarity. Neither did we attempt to correct for nonuniformity, variations in binomial p between the various release sites (Brown et al. 1976). Once we had an initial value of binomial p and n from *Eqs. 4* and *5*, we assumed that temporal variation in binomial n accounted for all the variance of the distribution.

Statistics

Most measurements were paired, one with and one without FMRF-NH_2. Data given in the text is shown as mean ± SE unless otherwise noted. We used a t test (t), a two-sample paired t test (t_s), or a Wilcoxon signed rank test T_s, to compare data sets (Sokal and Rohlf 1981).

Modeling

Computer programs for modeling were written in TURBO PASCAL v. 5.0 (Borland, Scotts Valley, CA). We used a stepsize control method incorporating a forward Euler step to determine an initial or "predicted" value. We then used a forward Trapezoidal step to determine a second or "corrected" value. If the predicted and corrected values were within a preset error limit, the step size was increased. If not, it was decreased.

RESULTS

Synaptic transmission between leech heart interneurons occurs at both hyperpolarized and depolarized holding potentials

When both heart interneurons in a reciprocally inhibitory pair were voltage clamped, the amplitude and time course of the postsynaptic currents depended on the holding potential of the presynaptic neuron. When a presynaptic heart interneuron was stepped from −70 to −35 mV, we observed an outward current in the postsynaptic cell (Fig. 1*A*). This outward current has been identified as a type of graded synaptic transmission (Angstadt and Calabrese 1991). Because this type of transmission occurs at hyperpolarized values of presynaptic membrane potential (−45 to −60 mV), we call it low-threshold transmission and it is associated with low-threshold Ca^{2+} currents extant in heart interneurons (Angstadt and Calabrese 1991).

When the presynaptic cell was held at −35 mV for durations of 3 s to 1.5 min and then stepped to 0 mV (Fig. 1*B*), there occurred an outward current in the postsynaptic neuron. This outward current presumably represents high-threshold transmission. At −35 mV, the low-threshold Ca^{2+} currents underlying low-threshold synaptic transmission are completely inactivated (Angstadt and Calabrese 1991).

High-threshold transmission produced postsynaptic currents that (*1*) were smaller in peak amplitude and (*2*) decayed more slowly than those produced by low-threshold transmission (Fig. 1).

The time course of the turn-on of the step-evoked postsynaptic current produced by high-threshold transmission had two components—fast and slow (Figs. 1*B* and 2*A*).

Both low-threshold and high-threshold transmission were observed between heart interneurons in over 30 experiments of this type.

FMRF-NH_2 alters the time course of step-evoked IPSCs

We examined the effect of FMRF-NH_2 on the time course of the postsynaptic current elicited by holding the presynaptic cell at −35 mV and stepping to either 0 or +5 mV for 250 ms. Steps were performed a minimum of 10 times on each preparation, and the currents evoked by the individual steps were averaged off-line.

As indicated, there were both fast and slow components of the time course of the turn-on the step-evoked IPSC. The time to peak of the fast component was 17.5 ± 1.93 (SE) ms (n = 7) (Fig. 2*A*). The time to peak of the slow component was 250 ± 28.5 ms (n = 8) (e.g., Fig. 3, *top panel*).

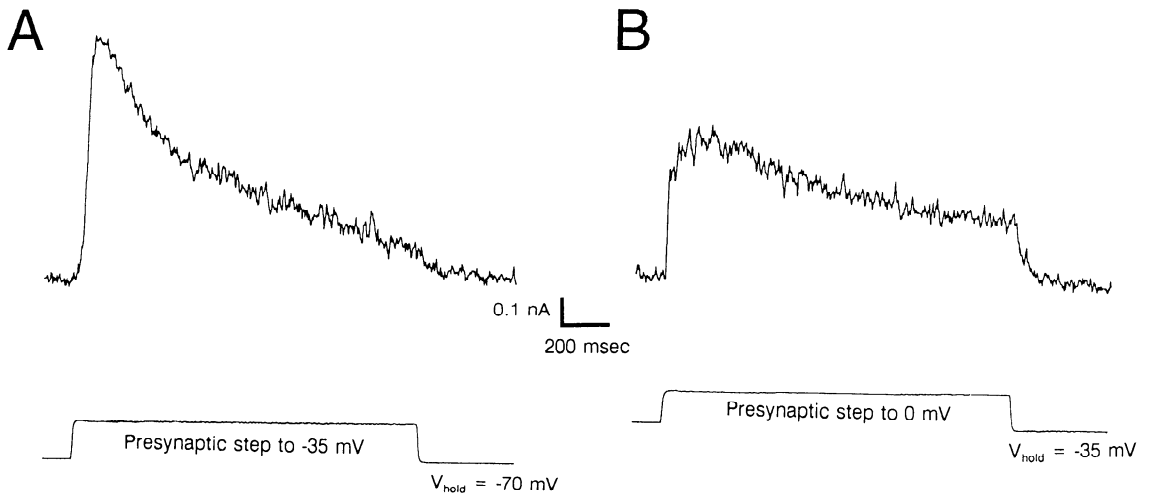

FIG. 1. Postsynaptic currents in a heart interneuron elicited from different holding potentials. *Top trace*: postsynaptic currents in cell HN(L,3); *bottom trace*: the simultaneous voltage in cell HN(R,3).

Bath-application of 1 μM FMRF-NH$_2$ either reduced or eliminated the fast component (e.g., Fig. 2*A*). In the absence of FMRF-NH$_2$, the amplitude of the fast component accounted for 41.5 ± 6.7% (n = 9, range: 0–67%) of the peak current evoked by a presynaptic voltage step to a saturating potential (> −10 mV). When the peptide was added, the amplitude of the fast component accounted for 23.7 ± 4.5% (n = 9, range: 0–47%) of the peak current. This reduction in the amplitude of the fast component was statistically significant (Wilcoxon signed rank test, $T_{s[9]}$ = 4, P < 0.025).

We define the turn-off of the IPSC as its waveform after the presynaptic voltage step has ended. We compared the time course of the turn-off of postsynaptic current evoked by short (200 ms) depolarizations in the presynaptic cell in the presence and absence of FMRF-NH$_2$ (Fig. 2*B*).

We attempted to fit the time course of the turn-off both to a single exponential and to two exponentials using in the linear least squares routine in the CLAMPFIT program of the PCLAMP software suite. The turn-off may contain a fast component that is unavailable because of the limited output bandwidth of our data acquisition system, and hence, we chose not to include the initial 10 ms of turn-off in these measurements. In all the preparations, the time course was better fit using a single exponential and the correlation coefficients (r) were all >0.9.

In five preparations, we measured the time constant of the turn-off from averaged data obtained in response to at least 10 presynaptic steps to +5 mV in the presence and absence of FMRF-NH$_2$. In all five cases the time constant was increased by application of FMRF-NH$_2$ (Fig. 2*B*). The average turn-off τ in the absence of FMRF-NH$_2$ was 25.99 ± 8.18 ms, and in its presence, the τ was 40.79 ± 10.97 ms ($t_{s[5,5]}$ = 2.42, P < 0.05).

The time course of the decay phase of the postsynaptic current is altered by FMRF-NH$_2$

After 200–400 ms of continued presynaptic depolarization (mean = 250 ± 28.5 [n = 8]), the IPSC began to decay even though the presynaptic depolarization was maintained [Figs. 1*B*, 3 (*top panel*) and 4]. This decay followed a single exponential time course (Fig. 4*A*). FMRF-NH$_2$ caused the decay of the IPSC to occur more rapidly (Fig. 4), and the acceleration of the decay time course caused a significant reduction in the IPSC amplitude after 700 ms during a 1500 ms presynaptic voltage step (Fig. 4B_1).

To examine further the effect of FMRF-NH$_2$ on the time course of IPSC decay, we measured the current amplitude at 100-ms intervals throughout the step and normalized these values to the peak current observed during the step to obtain the fraction of peak current at each interval. The use of this normalization procedure more clearly shows that FMRF-NH$_2$ accelerates the decay of the IPSC 500–800 ms after the start of the step.

FMRF-NH$_2$ alters both the amplitude and time course of spike-evoked IPSCs

We observed the effect of FMRF-NH$_2$ on IPSCs evoked by a spike in the presynaptic neuron six preparations. FMRF-NH$_2$ produced a highly significant decrease in the amplitude of the IPSC (Fig. 5, *A* and *B*; Table 2) ($t_{s[6,2]}$ = 3.03, P < 0.02). FMRF-NH$_2$ produced a significant increase in the time constant of the falling phase of the IPSC (Fig. 5, *A* and *B*) (Normal = 10.75 ± 1.24 ms, FMRF-NH$_2$ = 16.97 ± 2.59 ms, $t_{s[6,2]}$ = 2.23, P < 0.05).

We observed no consistent effect of FMRF-NH$_2$ on the width of presynaptic spikes or the size of the afterhyperpolarization.

One might expect spike broadening to occur in FMRF-NH$_2$ because it reduces the amplitude of I_K elicited from a holding potential of −35 mV (Simon et al. 1992). However, if spikes are passively conducted from a remote spike initiation site and the FMRF-NH$_2$-sensitive K$^+$ currents are somatic, the absence of spike broadening or no change in the afterhyperpolarization would be expected.

The amplitude of the postsynaptic current depends on the presynaptic potential

When the presynaptic neuron was depolarized from a holding potential of −35 mV under voltage clamp, postsynaptic currents first activated at a presynaptic potential of

−25 mV and reached a maximum between −10 and 0 mV (Fig. 6). The presence of FMRF-NH_2 had no consistent or significant effect on the peak amplitude of the step-evoked IPSC at presynaptic potentials < −10 mV. At presynaptic steps to 0 and +5 mV, FMRF-NH_2 produced a significant decrease in the peak amplitude (Fig. 6B_1).

The effect of FMRF-NH_2 on the decay time constant can be clearly seen (Fig. 6*A*, *right panel*). We measured the time integral of the step-evoked IPSC (Fig. 6B_2). As expected (cf. Fig. 4), FMRF-NH_2 produced a significant decrease in the magnitude of this integral at −5 and 0 mV.

High-threshold transmission is dependent on external Ca^{2+}

Similar to low-threshold graded transmission, high-threshold transmission between leech heart interneurons is dependent on external Ca^{2+}. Postsynaptic currents are reliably elicited by a 250-ms duration presynaptic voltage step from −35 to 0 mV (Fig. 7*A*) in the presence of 1.8 mM external Ca^{2+}. When the Ca^{2+} is replaced with Co^{2+}, high-threshold transmission disappears (Fig. 7*B*). Transmission reappears when Ca^{2+} is reintroduced into the superfusate (Fig. 7*C*).

We sometimes (2/4) observed a small inward current in the postsynaptic neuron when bathed in Co^{2+} saline during presynaptic voltage steps. This inward current may result from electrical coupling between the contralateral heart interneurons.

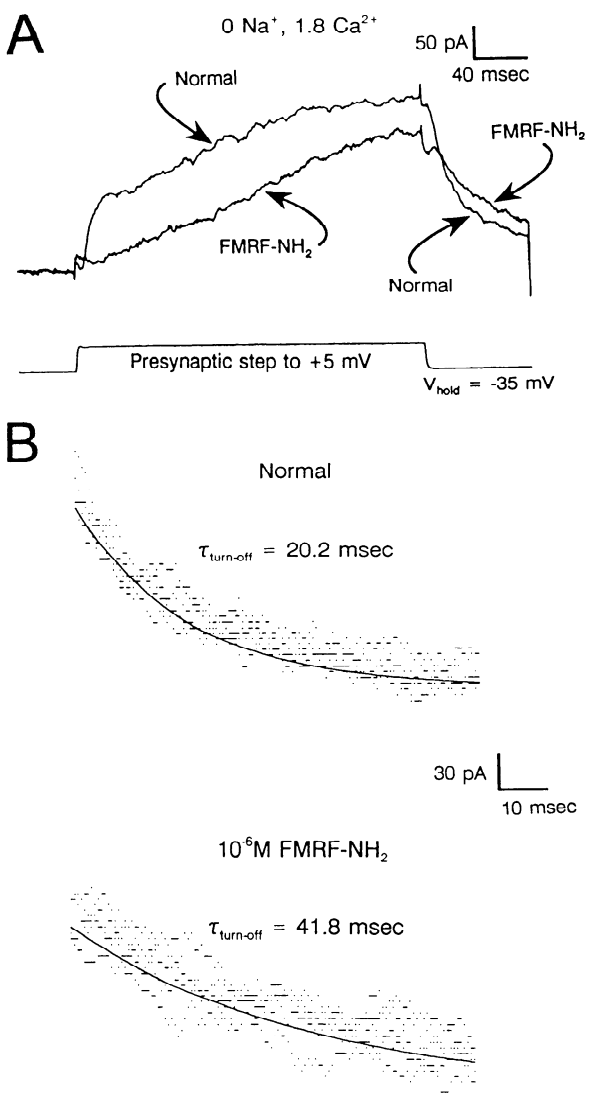

FIG. 2. Effect of FMRF-NH_2 on the time course of postsynaptic currents. *A*: averaged postsynaptic currents evoked by 250 ms presynaptic voltage steps to +5 mV before and after superfusing the preparation with 1 μM FMRF-NH_2. Each trace is the average of 12 individual steps. *B*: single exponential fits to the time constant of turn-off of the step-evoked current. The smooth line is the single exponential fit. The dots are 5 superimposed unaveraged traces.

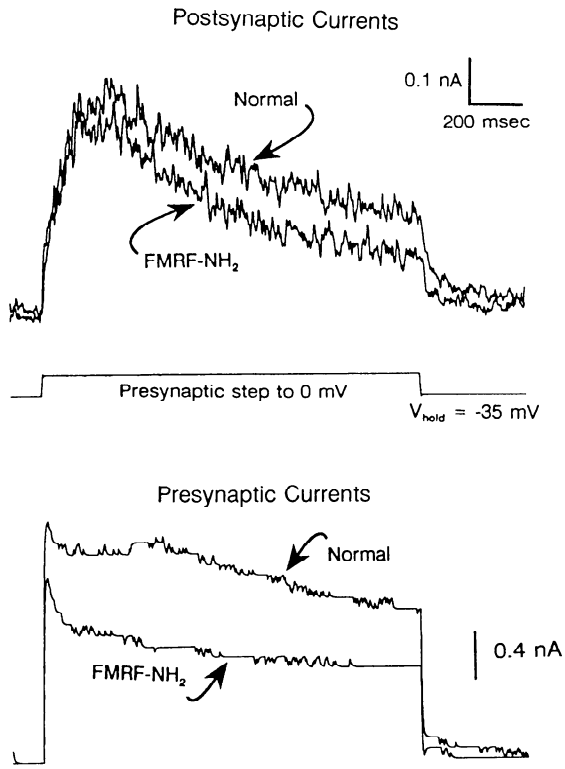

FIG. 3. Effect of FMRF-NH_2 on the postsynaptic currents evoked by 1.5-s duration presynaptic voltage steps. Postsynaptic currents (*top traces*) evoked by a presynaptic step (*middle trace*) to 0 mV. The presumed high-threshold Ca^{2+} current is masked by the large presynaptic outward currents (*bottom traces*). Note the reduction in the outward current, I_K, observed in the presence of FMRF-NH_2 (cf. Simon et al. 1992).

Quantal analysis of spike-mediated transmission and the effects of FMRF-NH_2 on binomial parameters

In five out of nine experiments, we obtained an array of IPSPs from a preparation in which the presynaptic cell was held at −50 mV. In all five cases at −50 mV, we observed either failures or release of single quanta (Fig. 8*A*; cf. Nicholls and Wallace 1978), and these experiments provided us an estimate of the unit size.

In all records, an artifact representing capacitative coupling between the two electrodes was present despite attempts at shielding. Nonetheless, the coupling artifact was of brief enough duration not to obscure the point of minimum latency we used as the baseline for measuring IPSP amplitude (Fig. 8*B*).

Noise was measured as indicated in MATERIALS AND METHODS. The noise histogram departed significantly from a normal distribution (χ^2 = 749.3, 159 df, $P < 0.001$),

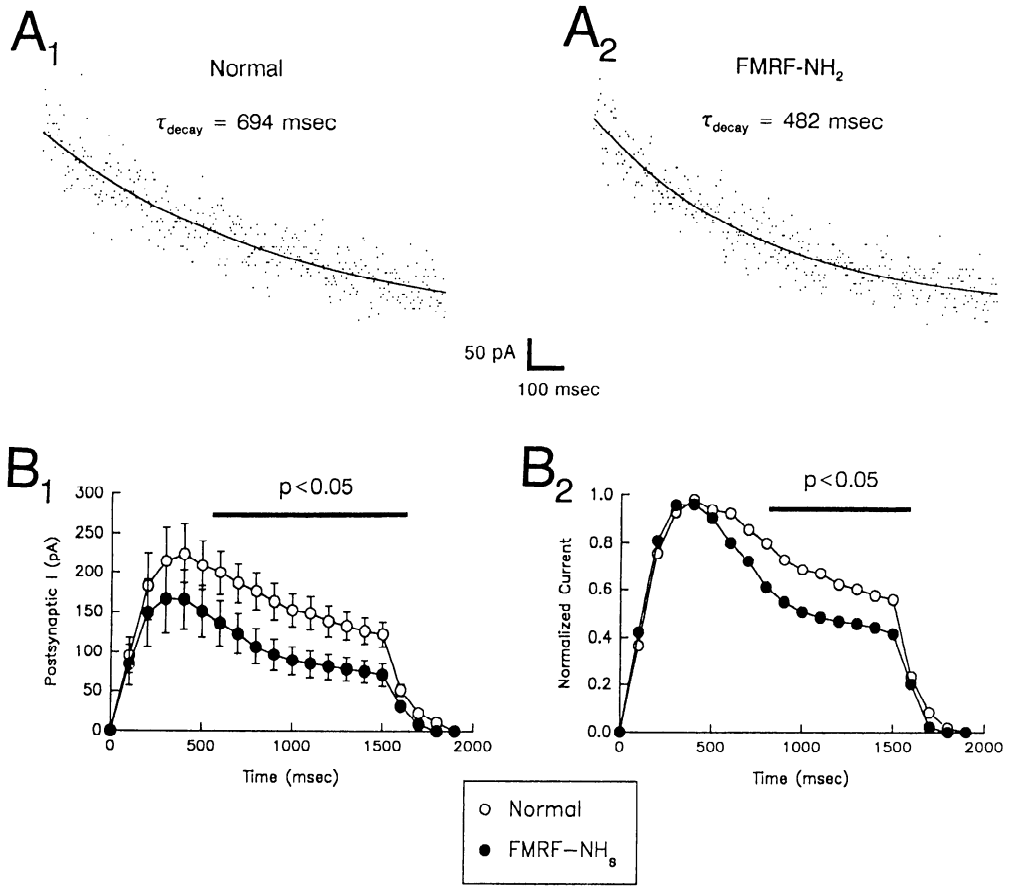

FIG. 4. Effect of FMRF-NH$_2$ on the decay time course of postsynaptic current evoked by 1.5-s duration presynaptic voltage steps. *A*: single exponential fits of decay time constants in the absence (A_1) and presence (A_2) of FMRF-NH$_2$. *B1*: average postsynaptic current evoked by a 1.5-s presynaptic voltage step. Each point is the mean of 8 experiments. Points are means ± SE. The bar above the graph indicates the times at which the differences were significant at the 5% level (paired *t* test). *B2*: average normalized current calculated from arcsine transforms (Sokal and Rohlf 1981) of the normalized current. Normalization of the current to the peak value reveals that the reduction of the inhibitory postsynaptic currents (IPSC) by FMRF-NH$_2$ occurs between 500 and 800 ms. Again, the bar above the graph indicates statistically significant differences between the normalized current amplitudes (paired *t* test).

which is plotted over the noise histogram (Fig. 8*C*). The noise had a trimodal distribution with a peak at 0.0 mV and peaks at ± 0.2 mV. These three peaks are observable in the distribution of IPSP amplitudes obtained from Expt. #6 with a presynaptic membrane potential of −50 mV (Fig. 8*A*). Only 10/128 values were significant outliers that departed from this trimodal noise distribution. Without any correction for the noise, the fits of our histograms were sufficiently good that we did not feel a deconvolution procedure was necessary (e.g., Edwards et al. 1976).

We examined the effect of FMRF-NH$_2$ on quantal synaptic transmission in nine preparations at a presynaptic holding potential of either −40, −35, or −30 mV. We used these particular holding potentials because the Ca^{2+} currents underlying low-threshold transmission would be completely inactivated. In some preparations, despite the addition of Mg^{2+} to the saline, spikes arose spontaneously and corrupted the records. The particular holding potential used in an experiment was the highest level at which spontaneous spikes were not problematic.

FMRF-NH$_2$ produced a significant increase in binomial *p*, the probability of release from 0.398 ± 0.038 to 0.507 ± 0.053 (Wilcoxon signed rank test, $T_{s[9]} = 3$, $P = 0.0098$). FMRF-NH$_2$ also produced a decrease in binomial *n* from 4.22 ± 0.74 to 2.22 ± 0.40 (Paired *t* test, $t_{s[9,2]} = 2.37$, $P = 0.03$). FMRF-NH$_2$ produced a significant decrease in *m*, quantal content, the product of *n* and *p* (*Eq. 3*), from 1.73 ± 0.35 to 1.10 ± 0.24 (Wilcoxon signed rank test, $T_{s[9]} = 0$, $P < 0.001$). The coefficients of variation (CV) were significantly increased by FMRF-NH$_2$ from 0.63 ± 0.06 to 0.79 ± 0.11 (Wilcoxon signed rank test, $T_{s[9]} = 3$, $P = 0.0098$). Data from four experiments are shown in Table 2, and an exemplar is shown in Fig. 9.

The unit size either determined by *Eq. 1* from experiments at a presynaptic potential of −50 mV or found by fitting the PSP distributions in the remaining four experiments was unchanged by application of FMRF-NH$_2$. The values for the unit size are shown in Table 3.

FMRF-NH$_2$ has no apparent effect on the postsynaptic neuron

The change in the CV and the lack of change in the unit size suggests that FMRF-NH$_2$ acts presynaptically to alter quantal parameters (Korn and Faber 1991). Acetylcholine has been shown to be the inhibitory transmitter between leech heart interneurons (Schmidt and Calabrese 1992),

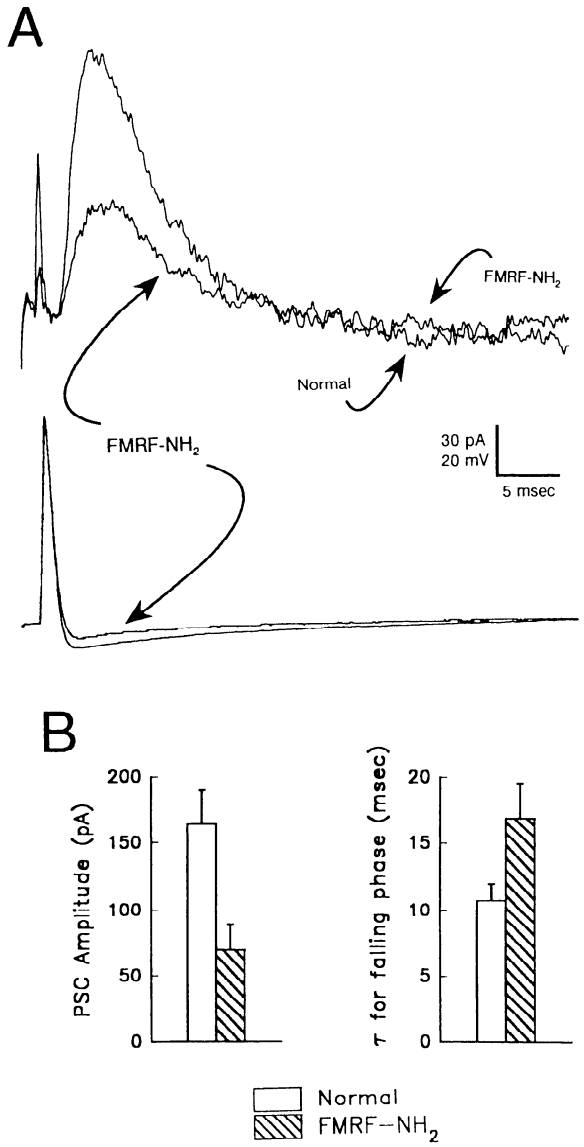

FIG. 5. Postsynaptic currents evoked by a spike in the presynaptic neuron. *A*: IPSCs in the postsynaptic neuron and spikes in the postsynaptic neuron in the presence and absence of FMRF-NH_2. *B*: bar graphs showing the effect of FMRF-NH_2 on the IPSC amplitude and the falling phase time constant.

and as a further test of the effect of FMRF-NH_2 on q, the unit size, we focally applied acetylcholine to the somata of heart interneurons with a picospritzer to produce an IPSP-like response (Fig. 10*A*). Superfusion of 1 μM FMRF-NH_2 produced no apparent change in either the amplitude or the integral of the IPSP-like response to focal ACh. We normalized both the amplitude and integral of the IPSP-like responses to the size of the control measures prior to superfusion. Washing the FMRF-NH_2 out produced no change in either the amplitude ($t_{5,2} = 0.67$, $P > 0.5$) or the integral ($t_{5,2} = 0.69$, $P > 0.5$) of the IPSP-like response (Fig. 10*B*).

The effects of FMRF-NH_2 on the spike-evoked IPSC suggests an indirect effect on I_h

In an oscillatory pair of heart interneurons, the critical timing transition is from the inhibited phase to the plateau/burst phase, i.e., from inactivity to activity. Thus one heart interneuron of an oscillatory pair can escape the inhibition of its contralateral homologue to enter the plateau/burst phase (Calabrese et al. 1989). The hyperpolarization-activated inward current, I_h, is an intrisic restorative force, which enables the escape from inhibition (Calabrese et al. 1989; Calabrese and DeSchutter 1992; DeSchutter et al. 1993b).

We used a computer model to examine the effect of FMRF-NH_2 altered IPSCs on I_h, the hyperpolarization-activated inward current (Angstadt and Calabrese 1989). A single heart interneuron was modeled as an isopotential compartment with a leak conductance of 11 nS, a leak equilibrium potential of −45 mV, and a capacitance of 500 pF (e.g., DeSchutter et al. 1993a,b). IPSCs were calculated as

$$I_{syn} = \overline{G_{syn}} \cdot (1 - e^{-t/\tau_{rise}}) \cdot e^{-t/\tau_{fall}} \quad (6)$$

The parameter $\overline{G_{syn}}$ was adjusted so that the amplitudes of the IPSC were −165 and −69 pA (Normal and FMRF-NH_2, respectively; Table 1). The rising time constant was taken to be 2.5 ms and the falling time constants were 10.75 and 16.97 ms (Normal and FMRF-NH_2, respectively; Table 1). IPSCs were administered to the model cell at frequencies between 5 and 25 Hz beginning 50 ms after the start of the simulation (Fig. 11). Because of the slow activation of I_h (~2 s), its familiar appearance as a "sag" voltage in apparent in these simulations (cf. Angstadt and Calabrese 1989; Calabrese et al. 1989).

We examined the slow increase of I_h in the model directly (Fig. 12*A*). I_h activated slowly over the first 2 s of the simulation and remained at a fairly constant level throughout the simulation. As one might expect, I_h is activated to a smaller extent when the effects of FMRF-NH_2-modulation of the IPSC were included in the simulation, but the reduction in I_h is slight (Fig. 12*A*; Table 4) with 80% as much current activated in FMRF-NH_2 as in the unmodulated state.

We calculated the Final Average Voltage by taking the mean of all simulated voltages during simulation time be-

TABLE 2. *Parameters of quantal transmission between leech heart interneurons*

Condition	V_{pre}	q	σ_q^2	CV	m	p	n
Normal	−35	0.38	0.016	0.556	2.29	0.29	8
FMRF-NH_2	−35	0.47	0.02	0.623	1.65	0.45	4
Normal	−40	0.4	0.012	0.648	1.20	0.49	2
FMRF-NH_2	−40	0.35	0.009	1.02	0.78	0.515	1
Normal	−30	0.322	0.01	0.333	3.46	0.58	6
FMRF-NH_2	−30	0.6	0.015	0.415	2.36	0.7	2
Normal	−30	0.6	0.02	0.376	4.56	0.504	7
FMRF-NH_2	−30	0.6	0.02	0.299	5.54	0.71	4

q, m, p, n, binomial parameters; CV, coefficient of variation.

TABLE 3. *Unit size calculated from failures or determined by fitting*

	Normal	FMRF-NH_2
$q_{failures}$	0.348 ± 0.082	0.346 ± 0.079
q_{fit}	0.428 ± 0.12	0.427 ± 0.10

Values are ± SE.

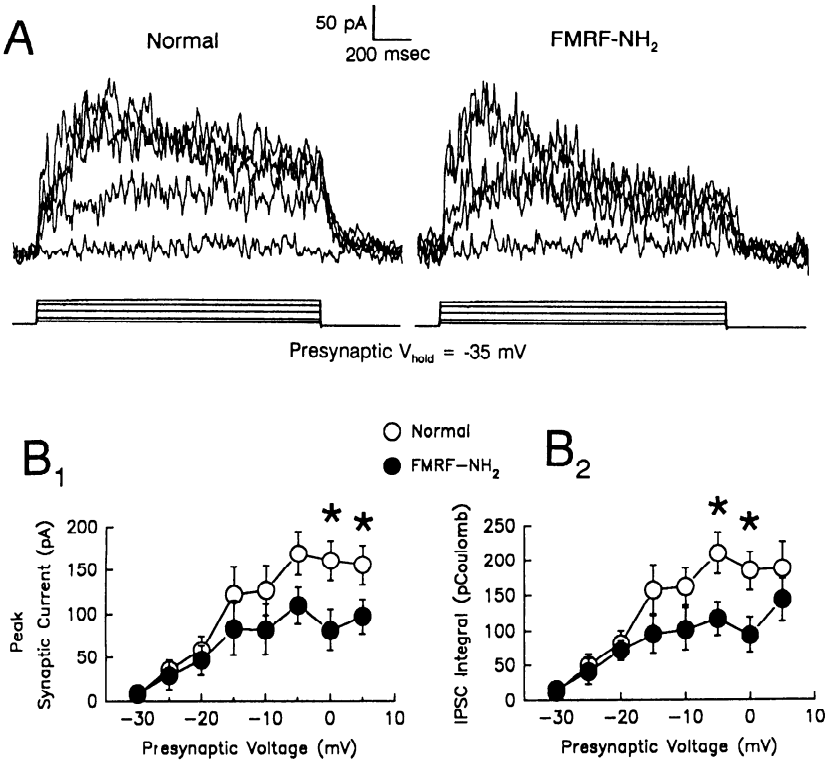

FIG. 6. Effect of presynaptic depolarization and FMRF-NH$_2$ on postsynaptic currents. *A*: step-evoked postsynaptic currents from presynaptic voltage steps to −30, −25, −15, −5, and +5 mV in the absence (*left panel*) and presence (*right panel*) of 1 μM FMRF-NH$_2$. B_1: peak postsynaptic current vs. presynaptic voltage. Each point is the mean of 5 preparations. The asterisks above values at 0 and +5 mV indicate a significant decrease in FMRF-NH$_2$ ($t_{s[5,2]} > 2.4$, $P < 0.05$). B_2: time integral of postsynaptic current vs. presynaptic voltage. Each point is the mean of 5 preparations. The asterisks above values at −5 and 0 mV indicate a significant decrease in FMRF-NH$_2$ ($t_{s[5,2]} > 2.3$, $P < 0.05$) Points are means ± SE.

tween 2,000 and 3,500 ms. The relationship between the Final Average Voltage and IPSC Frequency was linear and inversely proportional to frequency (Fig. 12B_1). We calculated the Final Average I_h in a similar way and found its relationship with IPSC Frequency was also linear and directly proportional (Fig. 12B_2).

We determined the peak IPSP by finding the minimum voltage between 50 ms simulation time (when the IPSC train began) and 2,000 ms. The peak IPSP decreased in a quadratic function with increasing IPSC frequency (Fig. 12B_3. See legend to Fig. 12 for these exact relationships).

DISCUSSION

A distinct Ca^{2+} current exists in leech heart interneurons and underlies high-threshold transmission

At a holding potential of −35 mV, the two low-threshold Ca^{2+} currents underlying graded synaptic transmission are completely inactivated (Angstadt and Calabrese 1991). That synaptic transmission occurs at this depolarized holding potential suggests the existence of a third Ca^{2+} current. Consistent with the existence of this high-threshold current is the absence of transmission in the presence of Co^{2+} (Fig. 7). It seems highly probable that the high-threshold transmission we have studied corresponds to spike-mediated transmission.

In this study, it has not been possible to examine this Ca^{2+} current directly while maintaining synaptic transmission because it is masked by the large competing outward currents elicited by depolarizing steps from −35 mV (Fig. 3, *bottom panel*, and Simon et al. 1992).

Adequacy of space clamp and voltage control of the dendrites of leech heart interneurons

If we assume that the presynaptic heart interneuron is not space clamped and poor voltage control exists in the dendrites, then the large presynaptic outward currents (Fig. 3, *bottom panel*) would tend to oppose the depolarizing step. During this step, the dendritic regions would be more hyperpolarized than the soma. If we assume that the high-

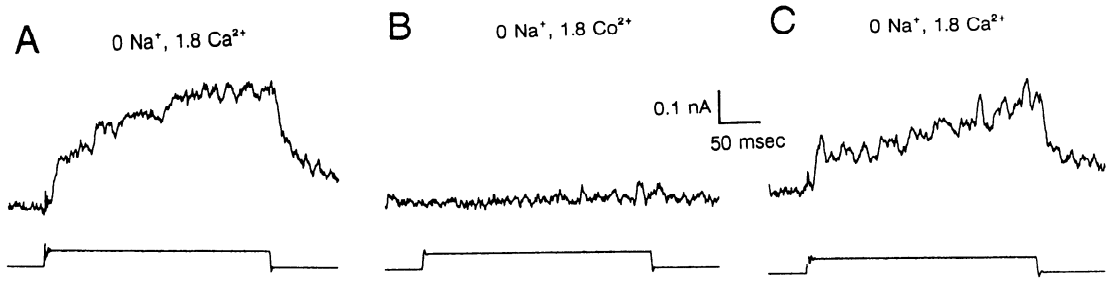

FIG. 7. Dependence of high-threshold transmission on external Ca^{2+}. *A*, *B*, and *C* were from the same preparation. *Top traces* are postsynaptic currents, and *bottom traces* are presynaptic voltage records. *A*: postsynaptic current evoked by a 250 ms presynaptic voltage step to 0 mV from a holding potential of −35 mV. As indicated, the preparation was superfused with 0 Na^+, 1.8 Ca^{2+}. *B*: synaptic transmission is blocked when the Ca^{2+} is replaced by an equimolar amount of Co^{2+}. *C*: transmission is restored when Ca^{2+} is re-added to the saline.

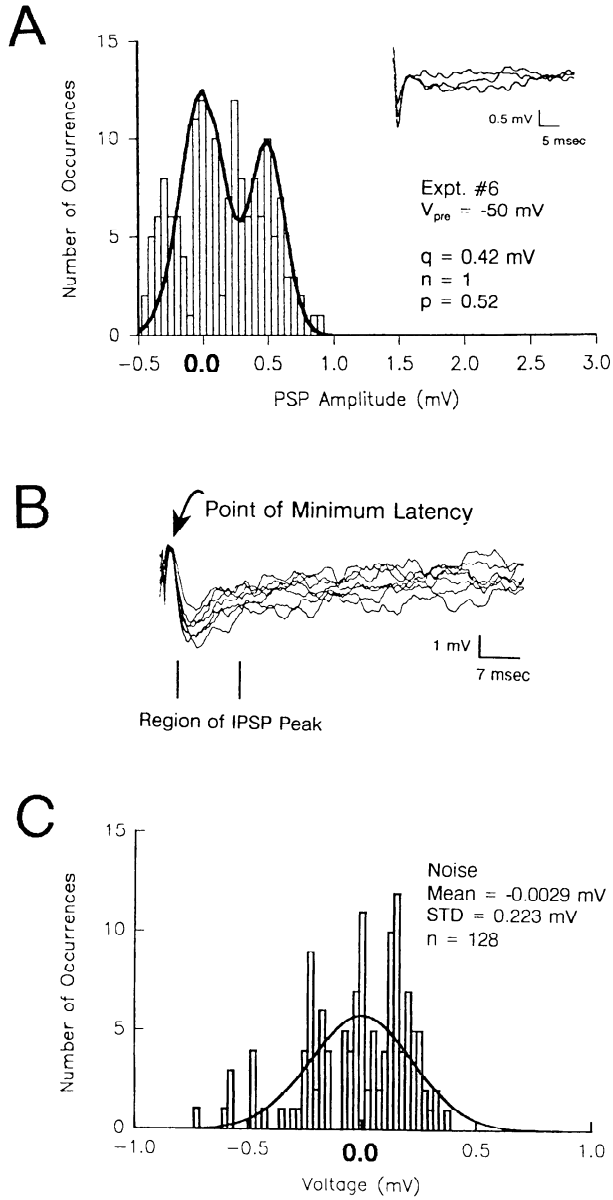

FIG. 8. Measurement of IPSPs for quantal analysis. *A*: histogram and fit of the IPSP array at a presynaptic potential of −50 mV. The inset shows a failure and 2 single quantum releases. *B*: seven superimposed IPSPs to show the point of minimum latency from which IPSP amplitude was measured. *C*: histogram and fit of noise from a pair of cells in which the presynaptic stimulation was subthreshold. The "zero" labels on the abscissa are in boldface for clarity.

threshold Ca^{2+} current increases with membrane depolarization, then, by reducing the amplitude of I_K (Simon et al. 1992 and Fig. 3), FMRF-NH_2 should cause the dendritic membrane potential to be more depolarized, and one would expect an increase in the postsynaptic current. Clearly, this is not observed in FMRF-NH_2 (Figs. 2, 3, and 5), and we have assumed that space clamp of these neurons is adequate.

Effects of FMRF-NH_2 on the spike-evoked IPSC

FMRF-NH_2 reduced the amplitude of all spike-evoked IPSCs (Fig. 5, *A* and *B*). Consistent with this is the reduction in amplitude of the fast component (Fig. 2*A*) of the high-threshold step-evoked IPSC evoked by a depolarizing step in a voltage-clamped presynaptic cell.

It took 200–400 ms for the IPSC to attain its peak amplitude when the presynaptic cell was depolarized under voltage clamp [Figs. 1*B*, 2*A*, and 3, (*top panel*)]. Because spikes last less than 10 ms, the IPSC evoked by a presynaptic spike (Fig. 5*A*) would reach only a low amplitude relative to that occurring 300 ms after the onset of a depolarizing step. The reduction in the amplitude of the spike-evoked IPSC produced by FMRF-NH_2 may result from the reduction of the fast component of the IPSC turn-on (Fig. 2*A*).

The reduction of the fast component is consistent with the reduction in binomial *n* (Fig. 9, Table 2).

FMRF-NH_2 may modulate the high-threshold Ca^{2+} current

The slowed falling phase time course of the spike-evoked IPSC and the increased τ of the turn-off of a step-evoked IPSC suggest that FMRF-NH_2 might produce alterations in the Ca^{2+} current underlying high-threshold transmission. In isolated cells of leech longitudinal muscle, FMRF-NH_2 appears to modulate a Ca^{2+} current (Norris and Calabrese 1990). In leech heart cells, FMRF-NH_2 modulates a Ca^{2+} current that first activates at ~ −20 mV (Thompson and Calabrese 1992), approximately the same presynaptic membrane potential at which we observe the onset of high-threshold transmission between leech heart interneurons. FMRF-NH_2 slows the rate of inactivation of this current with Ba^{2+} as the charge carrier in leech heart cells. If FMRF-NH_2 also slowed the rate of inactivation of the high-threshold Ca^{2+} current in heart interneurons, there would be more Ca^{2+} current remaining to deactivate and this would be reflected in the slower falling phase of a spike-evoked IPSC and the slower turn-off of a step-evoked IPSC.

The increase in binomial *p* (Fig. 9, Table 2) also indicates a possible modulatory effect of FMRF-NH_2 on the high-threshold Ca^{2+} current similar to its effect in leech heart cells (Thompson and Calabrese 1992). This effect may well be direct and not via modulation of I_K (cf. Simon et al. 1992).

The structural correlate of binomial n in heart interneurons

The number of dendrites and structural contacts between the two heart interneurons in an oscillatory pair far exceeds binomial *n* (Tolbert and Calabrese 1985). Generally, binomial *n* is believed to correspond to the number of loaded active zones (Hackett et al. 1989; Hackett and Buchheim 1984; Korn and Faber 1982; Zucker 1973). Perhaps each HN cell dendrite possesses only a single active zone, and binomial *n* represents the number of active dendrites. Perhaps a pool of dendrites are used for low-threshold graded transmission and a different pool is used for high-threshold transmission.

Effect of FMRF-NH_2 on binomial n and decay time course of the IPSC suggests an effect on transmitter mobilization

FMRF-NH_2 produced a significant reduction in binomial *n*, the number of units available for release, suggesting a decrease in mobilization of transmitter. Consistent with

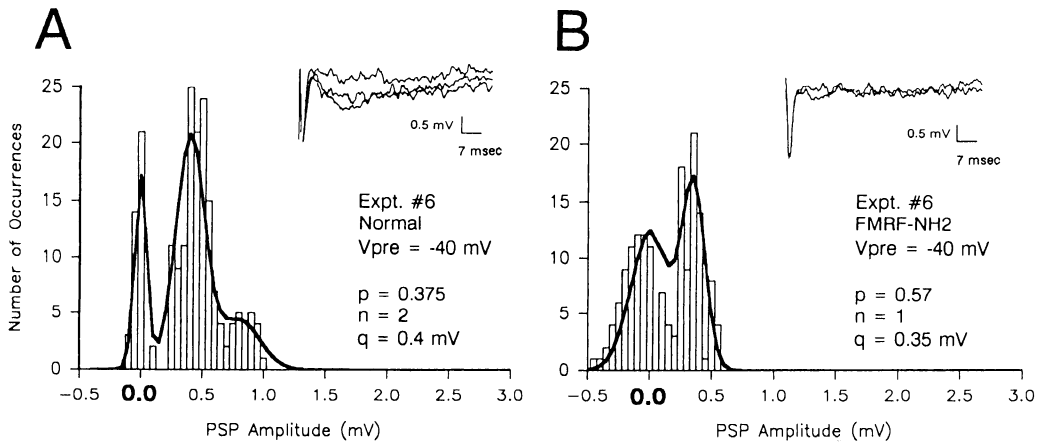

FIG. 9. Effect of FMRF-NH$_2$ on quantal synaptic transmission. *Left panel*: the histogram of IPSPs in the absence of FMRF-NH$_2$. The heavy line is the binomial fit calculated from the data in Table 1. The *inset* shows selected IPSPs from the distribution. The *right panel* shows a similar histogram from the same cell in the presence of FMRF-NH$_2$. The "zero" labels on the abscissa are in boldface for clarity.

this interpretation is the accelerated time course of decay of the IPSC evoked by long (1.5 s) steps in the presynaptic cell (Fig. 4).

The process of mobilization as a site of modulation of synaptic transmission was first proposed when models of synaptic modulation could not account for observed effects (Gingrich et al. 1988). Subsequently, a physiological mechanism underlying changes in mobilization has been observed in the activity of the protein synapsin I that binds to synaptic vesicles and to cytoskeletal structures and thus prevents the release of bound vesicles (Camillo and Greengard 1986).

The reduction in the fast component of the turn-on of step-evoked IPSC (Fig. 2*A*) is consistent with FMRF-NH$_2$ reduction of binomial *n*. If FMRF-NH$_2$ decreases the number of loaded active zones, then the time course of the slow component of the turn-on may represent the movement of vesicles from a storage pool close to the release site. The time-to-peak of the slow component was between 200 and 400 ms (Figs. 2 and 3). In a simulation of transmission in the gill withdrawal system of *Aplysia*, the time constant for mobilization was 213 ms (Gingrich and Byrne 1985), a value that would produce a similar time-to-peak to that which we observed.

The onset of the decay phase observed during 1.5 s presynaptic steps (Figs. 3 and 4*B*) may represent depletion of this nearby storage pool and reduced mobilization of vesicles from a further site of storage.

Effects of FMRF-NH$_2$ on spike-mediated transmission and I_K may account for both the disruptive and acceleratory effects of FMRF-NH$_2$ on the heart rhythm

In a previous paper (Simon et al. 1992), we reported a paradoxical effect of FMRF-NH$_2$ on the rhythm expressed by oscillatory pairs of heart interneurons. FMRF-NH$_2$ could either produce an acceleratory effect in which the rhythm speeded up, accompanied by an apparent decrease in transmission (Fig. 13 of Simon et al. 1992) or a disruptive effect in which transmission was abolished, and both neurons attained a potential close to that observed during a burst and continued to spike (Fig. 14 of Simon et al. 1992). There is evidence of a dosage effect of FMRF-NH$_2$ in producing these effects: lower concentrations of FMRF-NH$_2$

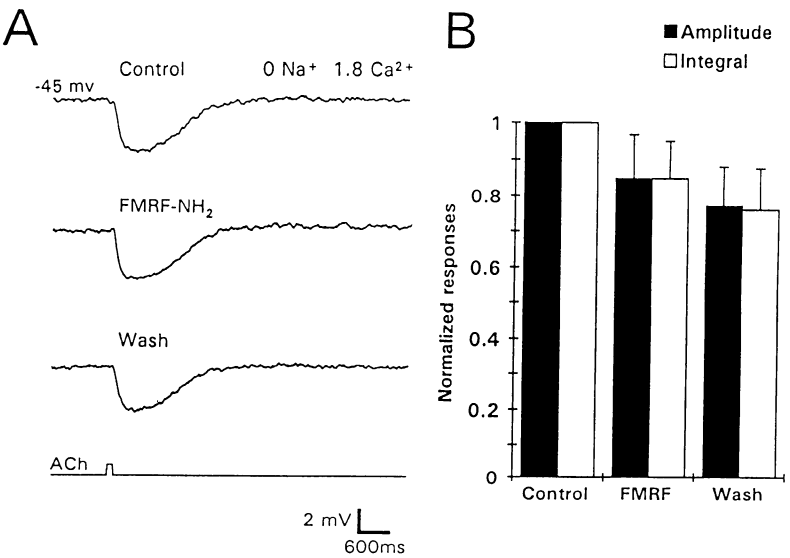

FIG. 10. Effect of FMRF-NH$_2$ on IPSP-like responses elicited by the application of exogenous transmitter. *A*: IPSP-like responses were elicited in an HN(4) interneuron by focal application of 10^{-3} M ACh in 0 Na^+, 1.8 Ca^{2+} saline. The heart interneurons were held at a membrane potential of −45 mV in discontinuous current clamp (DCC). Each trace is an average of 5 individual responses and was filtered with a time constant of 30 ms. *B*: amplitudes and integrals of IPSP-like responses were normalized to the levels measured prior to superfusion of FMRF-NH$_2$. Each bar is the average of 5 preparations (means ± SE).

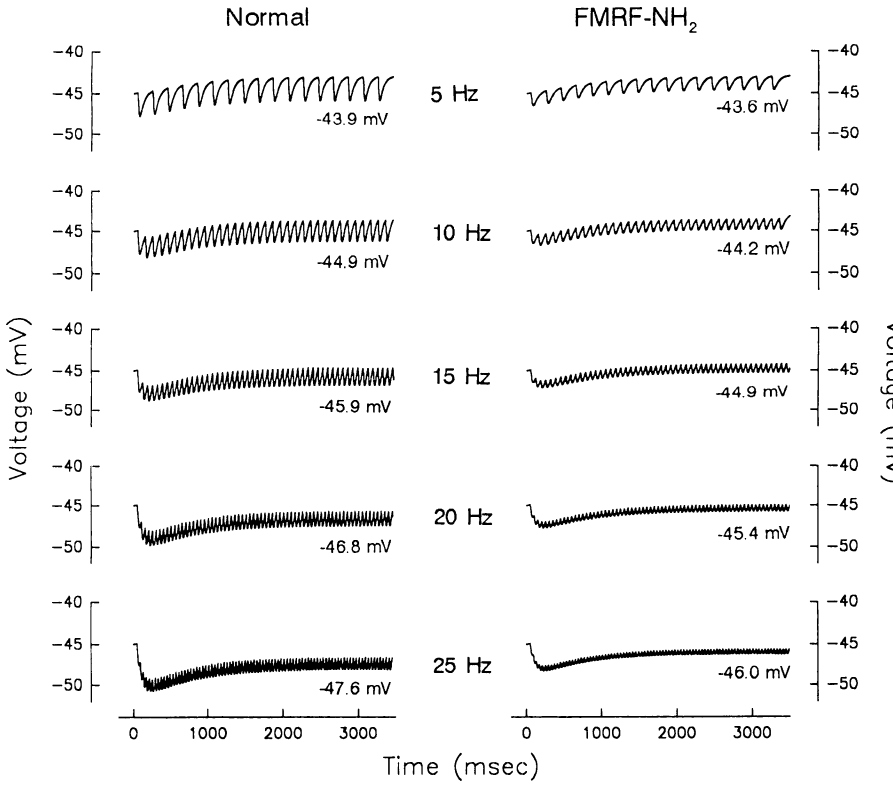

FIG. 11. Predicted effects of FMRF-NH_2 modulation of high-threshold transmission on I_h. The *left* column shows the simulated voltage responses of the model cell with IPSCs applied at frequencies ranging from 5 to 25 Hz. The *right* column shows the simulated voltage responses of the model cell with FMRF-NH_2-modulated IPSCs applied at similar frequencies. The number below each trace is the Final Average Voltage. (See text for details).

(10^{-9}–10^{-8} M) tend to produce an acceleratory response and higher concentrations of FMRF-NH_2 (10^{-7}–10^{-6} M) tend to produce a disruptive response (Kuhlman et al. 1985; Simon et al. 1992).

The disruptive response can be clearly explained by the reduction in amplitude of the spike-evoked IPSC by FMRF-NH_2 (Fig. 3). If transmission is sufficiently reduced, then the heart interneurons will never become sufficiently hyperpolarized to remove enough inactivation of the low-threshold calcium currents underlying graded transmission (Angstadt and Calabrese 1991); hence, there will be no plateaus and no sustained inhibition of the other neuron, necessary for I_h, the hyperpolarization-activated inward current (Angstadt and Calabrese 1989) to be activated and oscillation to occur.

Interactions between low-threshold Ca^{2+} currents and I_K at the beginning of the plateau/burst phase may also contribute to disruption (cf. Simon et al. 1992).

The model of the interaction of FMRF-NH_2 modulation of high-threshold transmission and I_h serves to explain the acceleratory response. When FMRF-NH_2 is present, the magnitude of the peak IPSP and the overall level of inhibition is less at all IPSC frequencies and the Final Average Voltage is more depolarized at all frequencies (Figs. 11 and 12B_1). Despite the decline in synaptic strength, I_h is activated to almost the same extent (Fig. 12A; Table 4) in the presence of FMRF-NH_2 as in its absence. Previously we had suggested that enhancement of I_h due to spike broadening and subsequent increased transmission might be the mechanism for the acceleratory response (Simon et al. 1992). We must now amend this to an *alteration* in transmission (i.e., changes in both amplitude and time course) that leads to very little change in I_h.

The critical timing transition in the oscillation of leech heart interneurons is escape from inhibition (Calabrese et al. 1989; Calabrese and DeSchutter 1992). Escape from inhibition depends directly on I_h. Thus the restorative force (I_h) is of almost equal magnitude in the presence or absence of FMRF-NH_2, but because the synaptic strength is less, I_h does not have to depolarize the cell over as large a voltage range to produce escape from inhibition.

Because the relationships of Final Average I_h and Final Average Voltage with IPSC frequency are linear (Fig. 12, B_1 and B_2), they change much less for a given change in frequency than does the peak IPSP whose relationship with IPSC frequency is quadratic (Fig. 12B_3). Hence, FMRF-NH_2-modulation has its greatest effect in reducing the peak IPSP, and this effect increases with increasing frequency (Fig. 12B_3).

We note that the spike rate is greatest ~500–1,000 ms after the peak of graded transmission when I_h is becoming strongly activated. Often in the presence of FMRF-NH_2, the spike rate is increased during this part of the cycle (Fig. 13 of Simon et al. 1992, *top trace*). Even though synaptic strength is reduced in FMRF-NH_2, the higher spike rate and increased summation of the FMRF-NH_2-modulated IPSPs would activate I_h possibly even more strongly than in the unmodulated state. In addition, the reduced amplitude of the IPSPs would tend to lower the range of membrane potential over which escape from inhibition by I_h would have to occur. Therefore, escape from inhibition would occur more rapidly in FMRF-NH_2, and acceleration of the heart rhythm would result.

In contrast to the usual role of action potentials, nondecrementing transmission of impulses over long distances, there is a local role for the burst of spikes in heart interneurons—shaping the rhythm of a single oscillatory pair. We have not observed an effect of FMRF-NH_2 on plateau-

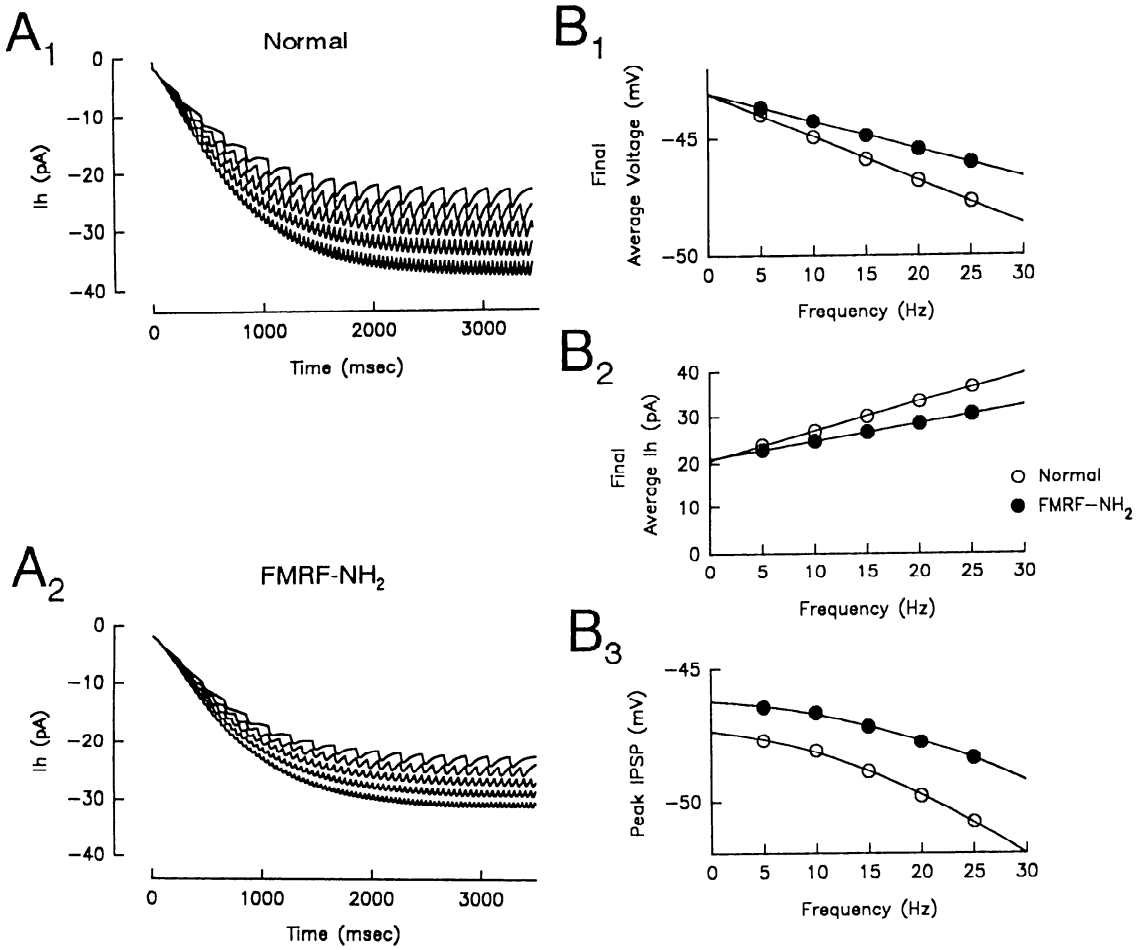

FIG. 12. Indirect effects of FMRF-NH$_2$ on I_h, membrane potential and the peak IPSP as revealed by the model. *A*: current trajectories for I_h during the simulation. A_1 the I_h trajectories with the normal synaptic parameters. A_2 the I_h trajectories with the FMRF-NH$_2$-modulated parameters. Records of IPSC frequencies from 5 to 25 Hz are shown. B_1: effect of FMRF-NH$_2$ modulation on the relationship of Final Average Voltage with IPSC frequency. These points were well fit by a linear relationship (linear regression, $r > 0.999$). For the normal case, the equation is

$$\text{Final Av. Voltage} = -43.056 - 0.182\,\phi \qquad (12.1)$$

and for FMRF-NH$_2$ modulation

$$\text{Final Av. Voltage} = -43.017 - 0.119\,\phi \qquad (12.2)$$

where ϕ is the IPSC frequency. B_2: effect of FMRF-NH$_2$ modulation on relationship of Final Average I_h with IPSC frequency. These points were well fit by a linear relation (linear regression, $r > 0.999$). For the normal case, the equation is

$$\text{Final Av. } I_h = 20.622 + 0.636\,\phi \qquad (12.3)$$

and for FMRF-NH$_2$ modulation,

$$\text{Final Av. } I_h = 20.974 + 0.382\,\phi \qquad (12.4)$$

B_3: effect of FMRF-NH$_2$ modulation on the relationship of the Peak IPSP with IPSC frequency. These points were well fit by a quadratic relationship (2nd order regression, $r > 0.999$). For the normal case, the equation is

$$\text{Peak IPSP} = -47.316 - 0.0481\,\phi - 0.00363\,\phi^2 \qquad (12.5)$$

and for FMRF-NH$_2$ modulation,

$$\text{Peak IPSP} = -46.222 - 0.0207\,\phi - 0.00263\,\phi^2 \qquad (12.6)$$

based oscillation (T. W. Simon, unpublished data) that occurs when external Ca^{2+} is raised and external Na^+ is lowered (Arbas and Calabrese 1984), indicating the presence of spikes is necessary for the effects of FMRF-NH$_2$ on the rhythm, nor does FMRF-NH$_2$ affect the low-threshold Ca^{2+} calcium currents (Angstadt and Calabrese 1991).

The most interesting part of these results is the fact that the changes in transmission that apparently result in acceleration of the heart rhythm are "matched" to the characteristics of both I_h and the low-threshold Ca^{2+} currents. Whether the accelcratory or disruptive response to bath-applied FMRF-NH$_2$ occurs may result from the extent to

TABLE 4. *Changes in final average I_h and peak IPSPs with IPSC frequency occurring with FMRF-NH_2-modulation*

IPSC Frequency	Percent Final Average I_h Remaining in FMRF-NH_2	Percent Peak IPSP Remaining in FMRF-NH_2
5	95.6	52.9
10	91.9	52.7
15	88.1	55.3
20	85.8	57.1
25	83.25	58.3

I_h, leak conductance.

which FMRF-NH_2 increases the duration of the IPSP (and thus indirectly enhances I_h) relative to the extent to which the peptide reduces the amplitude of the IPSP and causes more of the low-threshold Ca^{2+} currents to remain inactivated. We hope to incorporate details of the spike-evoked IPSCs into a model of the leech heartbeat pattern generator (e.g., DeSchutter et al. 1993a,b) and determine if the effect of FMRF-NH_2 on the high-threshold transmission can reproduce both the disruptive and acceleratory responses.

We thank Drs. Donald Edwards, Chuck Derby, and Cliff Opdyke for helpful discussions. We also thank Dr. Art English for the generous loan of equipment.

This work was supported by National Institute of Neurological Disorders and Stroke Grant NS-24072 to R. L. Calabrese and National Research Service Award Fellowship NS-08394 to T. W. Simon.

Address for reprint requests: R. L. Calabrese, Dept. of Biology, Emory University, 1510 Clifton Rd., Atlanta, GA 30322.

Received 27 January 1993; accepted in final form 13 September 1993.

REFERENCES

ANGSTADT, J. D. AND CALABRESE, R. L. Voltage clamp analysis of a hyperpolarization-activated inward current in heart interneurons of the medicinal leech. *J. Neurosci.* 9: 2846–2857, 1989.

ANGSTADT, J. D. AND CALABRESE, R. L. Calcium currents and graded synaptic transmission between heart interneurons of the leech. *J. Neurosci.* 11: 746–759, 1991.

ARBAS, E. A. AND CALABRESE, R. L. Rate modification in the heartbeat central pattern generator of the medicinal leech. *J. Comp. Physiol.* 155: 784–794, 1984.

BROWN, T. H., PERKEL, D. H., AND FELDMAN, M. W. Evoked neurotransmitter release: statistical effects of nonuniformity and nonstationarity. *Proc. Natl. Acad. Sci. USA* 73: 2913–2917, 1976.

CALABRESE, R. L. The neural control of alternate heartbeat coordination states in the leech, *Hirudo medicinalis*. *J. Comp. Physiol.* 122: 111–143, 1977.

CALABRESE, R. L., ANGSTADT, J. D., AND ARBAS, E. A. A neural oscillator based on reciprocal inhibition. In: *Perspectives in Neural Systems and Behavior*, edited by T. J. Carew and D. B. Kelley. New York: Alan R. Liss, 1989.

CALABRESE, R. L. AND DESCHUTTER, E. Motor-pattern-generating networks in invertebrates: modeling our way toward understanding. *Trends Neurosci.* 15: 439–445, 1992.

CAMILLO, P. D. AND GREENGARD, P. Synapsin I: a synaptic vesicle-associated neuronal phosphoprotein. *Biochem. Pharmacol.* 35: 4349–4357, 1986.

DESCHUTTER, E., ANGSTADT, J. D., AND CALABRESE, R. L. A model of graded synaptic transmission for use in dynamic network simulations. *J. Neurophysiol.* 69: 1225–1235, 1993a.

DESCHUTTER E., SIMON, T. W., ANGSTADT, J. D., AND CALABRESE, R. L. Modeling a neural oscillator that paces heartbeat in the medicinal leech. *Am. Zool.* 33: 16–28, 1993b.

EDWARDS, F. R., REDMAN, S. J., AND WALMSLEY, B. Statistical fluctuations in charge transfer at la synapses on spinal motoneurones. *J. Physiol. Lond.* 259: 665–688, 1976.

GINGRICH, K. J., BAXTER, D. A., AND BYRNE, J. H. Mathematical model of cellular mechanisms contributing to presynaptic facilitation. *Brain Res. Bull.* 21: 513–520, 1988.

GINGRICH, K. J. AND BYRNE, J. H. Simulation of synaptic depression, posttetanic potentiation, and presynaptic facilitation of synaptic potentials from sensory neurons mediating gill-withdrawal in *Aplysia*. *J. Neurophysiol.* 53: 652–669, 1985.

HACKETT, J. T. AND BUCHHEIM, A. Ultrastructural correlates of electrical-chemical synaptic transmission in goldfish cranial motor nuclei. *J. Comp. Neurol.* 224: 425–436, 1984.

HACKETT, J. T., COCHRAN, S. L., AND GREENFIELD, L. J. Quantal transmission at Mauthner axon target synapses in the goldfish brainstem. *Neuroscience* 32: 49–64, 1989.

JOHNSON, E. W. AND WERNIG, A. The binomial nature of transmitter release at the crayfish neuromuscular junction. *J. Physiol. Lond.* 218: 757–767, 1971.

KORN, H. AND FABER, D. S. Transmission at a central inhibitory synapse. II. Quantal description of release with a physical correlate for binomial *n*. *J. Neurophysiol.* 48: 679–707, 1982.

KORN, H. AND FABER, D. S. Quantal analysis and synaptic efficacy in the CNS. *Trends Neurosci.* 14: 439–445, 1991.

KUHLMAN, J. R., LI, C., AND CALABRESE, R. L. FMRF-amide-like substances in the leech: II. Bioactivity on the heartbeat system. *J. Neurosci.* 5: 2310–2317, 1985.

MACLACHLAN, E. M. The statistics of transmitter release at chemical synapses. *Int. Rev. Physiol. Neurophysiol. III* 17: 49–117, 1978.

NICHOLLS, J. G. AND WALLACE, B. G. Quantal analysis of transmitter release at an inhibitory synapse in the central nervous system of the leech. *J. Physiol. Lond.* 281: 171–185, 1978.

NORRIS, B. J. AND CALABRESE, R. L. Action of FMRFamide on longitudinal muscle of the leech, *Hirudo medicinalis*. *J. Comp. Physiol.* 167: 211–224, 1990.

PETERSON, E. L. Generation and coordination of heartbeat timing oscillation in the medicinal leech. I. Oscillation in isolated ganglia. *J. Neurophysiol.* 49: 611–626, 1983.

SCHMIDT, J. AND CALABRESE, R. L. Evidence that acetylcholine is an inhibitory transmitter of heart interneurons in the leech. *J. Exp. Biol.* 171: 329–347, 1992.

SIMON, T. W., OPDYKE, C. A., AND CALABRESE, R. L. Modulatory effects of FMRF-NH_2 on outward currents and oscillatory activity in heart interneurons of the medicinal leech. *J. Neurosci.* 12: 525–237, 1992.

SOKAL, R. R. AND ROHLF, F. J. *Biometry*, New York: Freeman, 1981.

THOMPSON, K. J. AND CALABRESE, R. L. FMRFamide effects on membrane properties of heart cells isolated from the leech, *Hirudo medicinalis*. *J. Neurophysiol.* 67: 280–291, 1992.

THOMPSON, W. J. AND STENT, G. S. Neuronal control of heartbeat in the medicinal leech. III. Synaptic relations of the heart interneurons. *J. Comp. Physiol.* 111: 281–307, 1976.

TOLBERT, L. P. AND CALABRESE, R. L. Anatomical analysis of contacts between identified neurons that control heartbeat in the leech, *Hirudo medicinalis*. *Cell Tissue Res.* 242: 257–267, 1985.

ZUCKER, R. S. Changes in the statistics of transmitter release during facilitation. *J. Physiol. Lond.* 229: 282–810, 1973.